Dalton Transactions

ROYAL SOCIETY OF CHEMISTRY

COMMUNICATION

View Article Online
View Journal | View Issue

Cite this: *Dalton Trans.*, 2025, **54**, 477

Received 14th October 2024,
Accepted 29th November 2024

DOI: 10.1039/d4dt02877e

rsc.li/dalton

Polyoxometalates as advanced-performance anions for ~D_{5h} Dy(III) single-ion magnets†

Ethan Lowe, Claire Wilson, Angelos B. Canaj * and Mark Murrie *

We enhance single-ion magnet (SIM) magnetisation reversal barriers by engineering the second coordination sphere, substituting conventional small monoanions with a bulky polyoxometalate (POM) trianion. Importantly, our approach serves as a model for creating new high-performance multifunctional hybrid materials.

Single-molecule magnets (SMMs) exhibit slow relaxation and retention of their magnetisation in the absence of a magnetic field.[1–3] Monometallic SMMs (or Single-Ion Magnets (SIMs)) can be designed by controlling the metal ion coordination environment to maximise the axial magnetic anisotropy.[4–6] The complexes with the highest energy barriers to magnetisation reversal (U_{eff}) and blocking temperatures contain lanthanide ions, in particular Dy(III).[7–10] Metallocene-based complexes have the highest blocking temperatures, although from a synthetic viewpoint the need for dry and inert atmospheres imposes more challenges on their crystal field engineering.[9,11–13] Therefore, when looking to enhance the performance of SIMs through synthetic modification, complex stability and synthetic flexibility are also highly desirable properties. The functionalisation and substitution of coordinating ligands have been shown to drastically change the magnetic properties of SIMs.[14,15] However, due to the fundamental importance of the lanthanide crystal field, changes to peripheral ligands, anions and non-coordinating solvents/ligands have a significant effect on the magnetic properties of SIMs.[16–19]

Previous work, in collaboration with Rajaraman's group, highlighted the potential to target the second coordination sphere to increase SIM magnetisation reversal barriers (U_{eff}).[19] This was done by using *in silico* models to remove the chloride anions, non-coordinating ligands and solvent from the crystal lattice of the pseudo-D_{5h} SIM $[Dy(H_2O^{eq})_5(HMPA^{ax})_2]Cl_3{\cdot}HMPA{\cdot}H_2O$ {eq = equatorial; ax = axial; HMPA = hexamethylphosphoramide}.[19] The chloride anions are located in the ~D_{5h} equatorial plane, hydrogen-bonded to the equatorial H_2O ligands and hence, they contribute to the transverse crystal field. In other words, they have a detrimental effect on the magnetic properties. Clearly, complete removal of the anions is impossible synthetically due to the disruption of the charge balance. Therefore, our idea was to substitute the three small chloride anions for a large, bulky trianionic polyoxometalate (POM) anion, to target (i) distancing the negative charge from the lanthanide centre; (ii) moving the negative charge out of the equatorial plane; (iii) increasing the distance between lanthanide centres and (iv) exploring the connection between the SIM properties and the surrounding environment.[20] Importantly, although the incorporation of polyoxometalates as anions has been proposed previously, all published compounds exclusively exhibit no appreciable U_{eff} barrier under zero applied magnetic field.[21]

Our first efforts to do this using our $[Dy(H_2O)_5(HMPA)_2]^{3+}$ complexes and phosphotungstic acid were hampered by synthetic issues, where we obtained either structural data that we couldn't fully refine or complexes with coordination of more than two HMPA ligands. Undeterred, we investigated a similar pseudo-D_{5h} complex containing axial P═O ligands $[Dy(H_2O^{eq})_5(Cy_3PO^{ax})_2]^{3+}$ {Cy_3PO = tricyclohexylphosphine oxide}.[22] We found that this complex, which contains a bulkier axial ligand, was stable in the presence of a POM anion and herein we report, for the first time, the synthesis, structural and magnetic characterisation of $[Dy(H_2O)_5(Cy_3PO)_2][W_{12}PO_{40}]{\cdot}2(Cy_3PO){\cdot}5THF{\cdot}H_2O$ (**1**). Importantly, we show that this new air-stable compound, containing a trianionic α-Keggin polyoxometalate, not only has the largest U_{eff} value in the $[Dy(H_2O)_5(Cy_3PO)_2]^{3+}$ family, but our approach opens the door to creating high-performance multifunctional hybrid compounds.

Compound **1** was synthesised using $[Dy(H_2O)_5(Cy_3PO)_2](CF_3SO_3)_3{\cdot}2(Cy_3PO)$ (**P1**) as the precursor in an anion substitution reaction.[18] A THF solution of **P1** along with

School of Chemistry, University of Glasgow, University Avenue, Glasgow, G12 8QQ, UK. E-mail: tsanai.angelos@gmail.com, mark.murrie@glasgow.ac.uk

†Electronic supplementary information (ESI) available: Experimental section, crystallographic details and magnetic studies. CCDC 2378028. For ESI and crystallographic data in CIF or other electronic format see DOI: https://doi.org/10.1039/d4dt02877e

$H_3[W_{12}PO_{40}]$, dissolved in a small amount of water, was heated and after workup, vapour diffusion using Et_2O yielded crystals of $[Dy(H_2O)_5(Cy_3PO)_2][W_{12}PO_{40}]\cdot 2(Cy_3PO)\cdot 5THF\cdot H_2O$ (**1**) where the three triflate anions in **P1** are replaced by a bulkier trianionic polyoxometalate (POM) anion (see ESI for synthesis and characterisation (Fig. S1)†). Importantly, we are the first to co-crystallise a high performance ~D_{5h} Dy(III) SIM with a POM anion whilst keeping the $\{Dy(H_2O^{eq})_5(L^{ax})_2\}$ unit intact. Compound **1** crystallises in the triclinic space group $P\bar{1}$ (Fig. 1). The Dy(III) centre exhibits a pentagonal bipyramidal geometry (~D_{5h}) as confirmed by continuous shape measures analysis (CShM = 0.204).[23] The axial Dy–O bond lengths are 2.208(9) and 2.210(10) Å, with the equatorial Dy–O bonds averaging 2.362(10) Å. The axial O–Dy–O angle of 176.3° and average equatorial O–Dy–O angle of 72.05° are close to the ideal values of 180° and 72°, respectively. The equatorial plane of $[Dy(H_2O)_5(Cy_3PO)_2]^{3+}$ is hydrogen bonded to four THF and one H_2O lattice solvents, two co-crystallised Cy_3PO molecules and two $[W_{12}PO_{40}]^{3-}$ anions (Fig. S2†). By replacing three small anions in **P1** with the large bulky POM trianion, the shortest intermolecular Dy···Dy distance increases from 12.6 Å in **P1** to 14.9 Å in **1**, leading to a better isolation of Dy(III) centres. The centre of the closest POM trianion lies 27.87° out of the $\{Dy(H_2O)_5\}$ equatorial plane and 9.83 Å away from the Dy(III) centre (see Fig. 1).

The magnetic properties of **1** constrained in eicosane were measured in an applied dc field of 1000 Oe from 280–2 K (Fig. S3†). Upon cooling $\chi_M T$ decreases steadily from 13.8 $cm^3\ mol^{-1}\ K$ to 12.4 $cm^3\ mol^{-1}\ K$ at 7 K, which precedes a sharp drop to 7.8 $cm^3\ mol^{-1}\ K$ at 2 K. The $\chi_M T$ value at 280 K is slightly lower than expected for a free Dy(III) ion (14.17 $cm^3\ mol^{-1}\ K$), which can be attributed to ligand field effects.[24,25] The sharp decrease in $\chi_M T$ at low temperatures is characteristic of a large magnetic anisotropy.[19] The zero-field cooled and field cooled magnetic susceptibility of **1** diverges at 8 K, with a clear maximum observed at 4.5 K (Fig. S5†). Hysteresis measurements at a sweep rate of 200 Oe s^{-1} show open, waist-restricted, loops at zero field. This is a common feature amongst ~D_{5h} SIMs due to the presence of unsuppressed quantum tunnelling of the magnetisation (QTM), which arises due to distortions from D_{5h} symmetry, introducing non-axial crystal field terms.[26–28] Compound **1** exhibits a blocking temperature ($T_{B(Hyst)}$) of 12 K (Fig. 2).

Alternating current (ac) magnetic susceptibility measurements show well-defined maxima in χ''_M *vs.* T up to 35 K for **1** (Fig. S6†). Large increases in χ''_M are observed at low temperatures, further indicating efficient QTM, which has been observed for a number of pseudo-D_{5h} complexes of general formula $[Dy(H_2O^{eq})_5(L^{ax})_2]^{3+}$ (Fig. 3).[18,19,27] The relaxation times τ were determined using the Cole–Cole plots of χ''_M *vs.* χ'_M *via* CCFIT2, using a generalized Debye model[29,30] (see Fig. S8 and S11†). In plotting τ^{-1} *vs.* temperature, relaxation parameters were obtained by fitting the data using the equation $\tau^{-1} = \tau_{QTM}^{-1} + CT^n + \tau_0^{-1}e^{\left(-\frac{U_{eff}}{T}\right)}$ for **1**, at zero applied field (Fig. 4) and $\tau^{-1} = CT^n + \tau_0^{-1}e^{\left(-\frac{U_{eff}}{T}\right)}$ under a 1000 Oe applied field (see Fig. S11†).

Under zero applied dc field, the τ values for **1** were fitted over the temperature range 3–35 K giving U_{eff} = 625(1) K, τ_0 = 4.6(5) × 10^{-12} s, C = 2.9(13) × 10^{-4} $K^{-n}\ s^{-1}$, n = 3.4(1) and

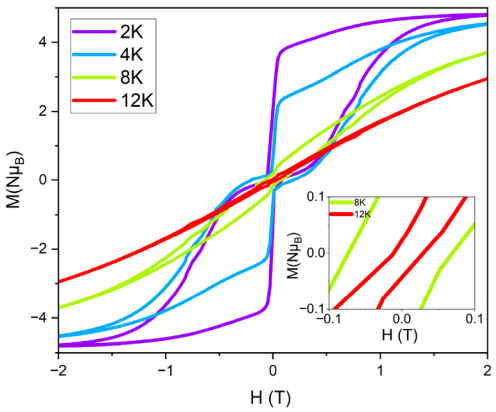

Fig. 2 Magnetic hysteresis measurements for **1** with a sweep rate of 200 Oe s^{-1}.

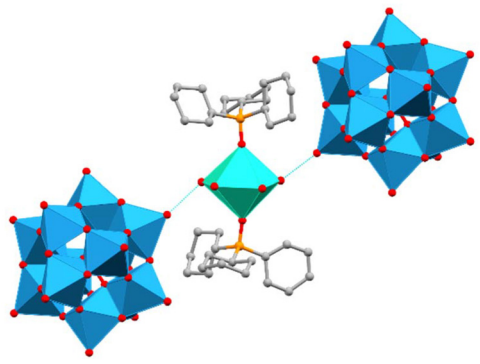

Fig. 1 The relative position of the POM anions to the Dy complex in $[Dy(H_2O)_5(Cy_3PO)_2][W_{12}PO_{40}]$ with solvent, co-crystalised Cy_3PO and H atoms omitted for clarity (only one POM anion is present within the asymmetric unit). C, grey; Dy, cyan; O, red; P, orange; W, blue.

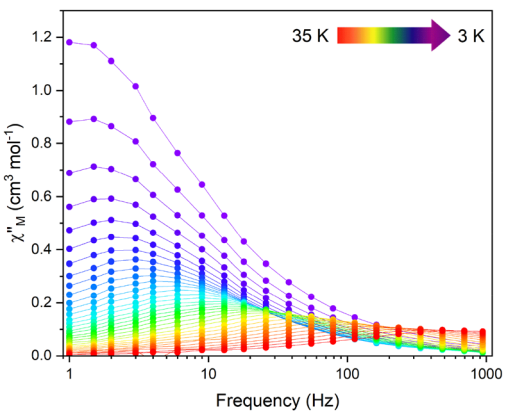

Fig. 3 Frequency dependence of the out-of-phase (χ''_M) magnetic susceptibility, under zero dc field, for **1** from 35–3 K.

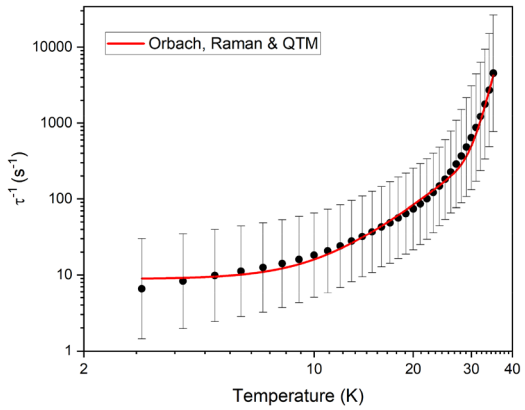

Fig. 4 Temperature dependence of the relaxation rate for **1** without an applied dc field. The solid line represents the best fit to Orbach, Raman and QTM relaxation (see text for details). Black vertical bars are estimated standard deviations in the relaxation times derived from Debye fits according to ref. 29.

τ_{QTM}^{-1} = 8.9(6) s^{-1}. The Orbach parameters obtained are consistent with those obtained under a 1000 Oe applied field where U_{eff} = 621(6) K, $\tau_0 = 5.0(8) \times 10^{-12}$ s (Fig. S11†). The U_{eff} observed for **1** (625 K) is the highest magnetisation reversal barrier observed within the $[Dy(H_2O)_5(Cy_3PO)_2]^{3+}$ family (see Table 1) indicating that the incorporation of the polyoxometalate has a significant effect on the magnetic behaviour. At this time, we are unable to carry out CASSCF calculations on **1** due to the large size and nature of this system, as also noted recently by Kong *et al.*[21]

In order to investigate the effects of incorporating the POM anion, **1** has been compared to other $[Dy(H_2O)_5(Cy_3PO)_2]X_3$ compounds, with different axial O–$\widehat{Dy}$–O angles and pentagonal bipyramidal CShM values (see Table 2). Between all complexes, the axial and equatorial Dy–ligand bonds vary by only 0.032 Å and 0.010 Å, respectively, allowing us to disregard this as a reason for the increase in U_{eff}. A comparison of **1** to compound **C1**, which has similar axial O–$\widehat{Dy}$–O angles (176.3° *vs.* 175.8°) and CShM values (0.204 *vs.* 0.239), allows us to focus on the large increase in the Dy–anion distance (4.59 *vs.* 9.83 Å) and the increased $\{Dy(H_2O)_5\}$ plane–anion angle (4.22 *vs.* 27.87°). These increases will result in a decrease in the transverse field contribution[19] by the POM anion and are accompanied by a large increase in U_{eff} (of 153 K). Whilst a change in hydrogen bonding is expected to alter the relaxation dynamics, rationalisation of the effects is not trivial. A full comparison with the other compounds offers no correlation with U_{eff} or $T_{B(Hyst)}$ and can be found in Table S2.†[19,31] We note that an increase in U_{eff} has also been observed upon diamagnetic dilution in another ~D_{5h} system.[32] Remarkably, the large U_{eff} observed in **1** exceeds that of **C2** (543 K) which has near linear axial O–$\widehat{Dy}$–O angle of 179° and a CShM of 0.142. However, the large U_{eff} associated with **1** does not translate to the persistence of hysteresis loops above temperatures reported for **C2**, highlighting the necessity to consider through the barrier mechanisms such as Raman and QTM, noting that the L^{ax}–Dy–L^{ax} linearity is an integral factor in designing high performance SIMs.[6,33]

When measuring slow magnetic relaxation, the primary method for the separation of Ln(III) SIMs focusses on doping the paramagnetic complex into a diamagnetic host. Here we demonstrate an alternative strategy for designing better separated Dy(III) systems by focussing on the anions present. Importantly, this approach may be especially relevant when doping into a diamagnetic host is too complicated or even impossible. By engineering the secondary coordination sphere of $[Dy(H_2O)_5(Cy_3PO)_2]^{3+}$, replacing three small anionic ligands

Table 1 A comparison of U_{eff}, τ_0 and $T_{B(Hyst)}$ for **1** and other $[Dy(H_2O)_5(Cy_3PO)_2]^{3+}$ SIMs

Complex	U_{eff} (K)	τ_0 (s)	$T_{B(Hyst)}$ (K) (200 Oe s^{-1})
$[Dy(Cy_3PO)_2(H_2O)_5]Cl_3$ $(Cy_3PO)\cdot H_2O\cdot EtOH$ **C1** [21]	472(7)	8.7×10^{-12}	11
$[Dy(Cy_3PO)_2(H_2O)_5]Br_3 \cdot 2(Cy_3PO)\cdot 2H_2O\cdot 2EtOH$ **C2** [21]	543(2)	2.0×10^{-11}	20
$[Dy(H_2O)_5(Cy3PO)_2](CF_3SO_3)_3 \cdot 2(Cy3PO)$ **P1** [18]	562(7)	$1.7(5) \times 10^{-11}$	n/a
1 This work	625(1)	$4.6(5) \times 10^{-12}$	12

Table 2 A comparison of selected bond lengths, angles and CshMs values for **1** and other $[Dy(H_2O)_5(Cy_3PO)_2]^{3+}$ SIMs in the literature

Compound	Dy–O_{ax} (Å)	Average Dy–O_{eq} (Å)	CShM PBPY-7 (D_{5h})	O–$\widehat{Dy}$–O angle (°)	Dy···Dy intermolecular distance (Å)	Dy–anion distance (Å)	$\{Dy(H_2O)_5\}$ plane–anion angle (°)
$[Dy(Cy_3PO)_2(H_2O)_5]Cl_3\cdot(Cy_3PO)\cdot H_2O\cdot EtOH$ **C1** [21]	2.217(4), 2.221(4)	2.359(5)	0.239	175.8(1)	8.420	4.59	4.22
$[Dy(Cy_3PO)_2(H_2O)_5]Br_3\cdot 2(Cy_3PO)\cdot 2H_2O\cdot 2EtOH$ **C2** [21]	2.189(3), 2.210(3)	2.352(3)	0.142	179.0(1)	11.23	4.77	4.42
$[Dy(H_2O)_5(Cy_3PO)_2](CF_3SO_3)_3\cdot 2(Cy_3PO)$ **P1** [18]	2.202(2), 2.203(2)	2.362(3)	0.639	173.4(1)	12.64	5.38[a]	1.48[a]
1 This work	2.208(9), 2.210(10)	2.362(10)	0.204	176.3(4)	14.89	9.83[b]	27.87[b]

[a] S atoms of the triflate anion used. [b] Centre of the polyoxometalate anion used.

with a large bulky trianion, we have successfully implemented the design criteria previously laid out,[19] to improve the U_{eff} energy barrier in this ~D_{5h} system. Specifically, by incorporating a polyoxometalate anion we have designed a new hybrid compound achieving both the largest U_{eff} barrier and $T_{B(Hyst)}$ of any POM containing SIM. Several compounds have been synthesised in recent years with POMs as anions (see Table S3†) or ligands (see Table S4†). However, the landmark compound **1** exhibits a U_{eff} over six times larger than any compound containing a POM anion, which opens up the possibility of new high-performance hybrid compounds. Considering the numerous applications and fascinating properties of POMs, this research also opens the door to a vast array of new multifunctional materials.

Data availability

Crystallographic data for **1** have been deposited under CCDC 2378028† and can be obtained from **https://www.ccdc.cam.ac.uk/structures/**.

Conflicts of interest

There are no conflicts to declare.

Acknowledgements

We thank EPSRC UK (EP/T517896/1) for funding and the EPSRC UK National Crystallography Service at the University of Southampton for the collection of the crystallographic data.[34] We thank Professor Gopalan Rajaraman for helpful discussions.

References

1 D. N. Woodruff, R. E. P. Winpenny and R. A. Layfield, *Chem. Rev.*, 2013, **113**, 5110–5148.
2 M. J. Giansiracusa, G. K. Gransbury, N. F. Chilton and D. P. Mills, *Single-Molecule Magnets, Encyclopedia of Inorganic and Bioinorganic Chemistry*, Wiley, 2021, pp. 1–21.
3 R. A. Layfield and M. Murugesu, *Lanthanides and Actinides in Molecular Magnetism*, John Wiley & Sons, 2015.
4 J. D. Rinehart and J. R. Long, *Chem. Sci.*, 2011, **2**, 2078–2085.
5 G. A. Craig and M. Murrie, *Chem. Soc. Rev.*, 2015, **44**, 2135–2147.
6 S. K. Gupta and R. Murugavel, *Chem. Commun.*, 2018, **54**, 3685–3696.
7 H. L. C. Feltham and S. Brooker, *Coord. Chem. Rev.*, 2014, **276**, 1–33.
8 C. Benelli and D. Gatteschi, *Chem. Rev.*, 2002, **102**, 2369–2388.
9 F.-S. Guo, B. M. Day, Y.-C. Chen, M.-L. Tong, A. Mansikkamäki and R. A. Layfield, *Science*, 2018, **362**, 1400–1403.
10 A. Dey, P. Kalita and V. Chandrasekhar, *ACS Omega*, 2018, **3**, 9462–9475.
11 S.-D. Jiang, B.-W. Wang, H.-L. Sun, Z.-M. Wang and S. Gao, *J. Am. Chem. Soc.*, 2011, **133**, 4730–4733.
12 C. A. P. Goodwin, F. Ortu, D. Reta, N. F. Chilton and D. P. Mills, *Nature*, 2017, **548**, 439–442.
13 C. A. Gould, K. R. McClain, D. Reta, J. G. C. Kragskow, D. A. Marchiori, E. Lachman, E.-S. Choi, J. G. Analytis, R. D. Britt, N. F. Chilton, B. G. Harvey and J. R. Long, *Science*, 2022, **375**, 198–202.
14 K.-X. Yu, J. G. C. Kragskow, Y.-S. Ding, Y.-Q. Zhai, D. Reta, N. F. Chilton and Y.-Z. Zheng, *Chem*, 2020, **6**, 1777–1793.
15 R. Liu, C. Zhang, L. Li, D. Liao and J.-P. Sutter, *Dalton Trans.*, 2012, **41**, 12139–12144; A. B. Canaj, S. Dey, O. Céspedes, C. Wilson, G. Rajaraman and M. Murrie, *Chem. Commun.*, 2020, **56**, 1533–1536; A. B. Canaj, M. K. Singh, E. Regincós Martí, M. Damjanović, C. Wilson, O. Céspedes, W. Wernsdorfer, G. Rajaraman and M. Murrie, *Chem. Commun.*, 2019, **55**, 5950–5953; R. Stewart, A. B. Canaj, S. Liu, E. Regincós Martí, A. Celmina, G. Nichol, H.-P. Cheng, M. Murrie and S. Hill, *J. Am. Chem. Soc.*, 2024, **146**, 11083–11094.
16 K. S. Pedersen, L. Ungur, M. Sigrist, A. Sundt, M. Schau-Magnussen, V. Vieru, H. Mutka, S. Rols, H. Weihe, O. Waldmann, L. F. Chibotaru, J. Bendix and J. Dreiser, *Chem. Sci.*, 2014, **5**, 1650–1660.
17 S. K. Gupta, S. Dey, T. Rajeshkumar, G. Rajaraman and R. Murugavel, *Chem. – Eur. J.*, 2022, **28**, e202103585.
18 I. F. Díaz-Ortega, J. M. Herrera, S. Dey, H. Nojiri, G. Rajaraman and E. Colacio, *Inorg. Chem. Front.*, 2020, **7**, 689–699.
19 A. B. Canaj, M. K. Singh, C. Wilson, G. Rajaraman and M. Murrie, *Chem. Commun.*, 2018, **54**, 8273–8276.
20 A. P. Orlova, M. S. Varley, M. G. Bernbeck, K. M. Kirkpatrick, P. C. Bunting, M. Gembicky and J. D. Rinehart, *J. Am. Chem. Soc.*, 2023, **145**(40), 22265–22275.
21 C. Hu, Y.-L. Lu, Y.-Z. Li, Y.-P. Yang, M. Liu, J.-M. Liu, Y.-Y. Li, Q.-H. Jin and Y.-Y. Niu, *Environ. Res.*, 2022, **206**, 112267; L. Wang, W. Yang, F.-Y. Yi, H. Wang, Z. Xie, J. Tang and Z.-M. Sun, *Chem. Commun.*, 2013, **49**, 7911; W. Zhou, X. Feng, H. Ke, Y. Li, J. Tang and E. Wang, *Inorg. Chim. Acta*, 2013, **394**, 770–775; H. Kong, Z.-Y. Ruan, Y.-C. Chen, W. Deng, P.-Y. Liao, S.-G. Wu and M.-L. Tong, *Inorg. Chem.*, 2024, **63**, 15964–15972.
22 Y.-C. Chen, J.-L. Liu, L. Ungur, J. Liu, Q.-W. Li, L.-F. Wang, Z.-P. Ni, L. F. Chibotaru, X.-M. Chen and M.-L. Tong, *J. Am. Chem. Soc.*, 2016, **138**, 2829–2837; A. M. J. Lees and A. W. G. Platt, *Polyhedron*, 2014, **67**, 368–372.
23 M. Pinsky and D. Avnir, *Inorg. Chem.*, 1998, **37**, 5575–5582.

24 D. Parker, E. A. Suturina, I. Kuprov and N. F. Chilton, *Acc. Chem. Res.*, 2020, **53**, 1520–1534.
25 E. Regincós Martí, A. B. Canaj, T. Sharma, A. Celmina, C. Wilson, G. Rajaraman and M. Murrie, *Inorg. Chem.*, 2022, **61**, 9906–9917.
26 S. T. Liddle and J. van Slageren, *Chem. Soc. Rev.*, 2015, **44**, 6655–6669.
27 Y. Ding, N. F. Chilton, R. E. Winpenny and Y. Zheng, *Angew. Chem., Int. Ed.*, 2016, **55**, 16071–16074.
28 A. B. Canaj, S. Dey, C. Wilson, O. Céspedes, G. Rajaraman and M. Murrie, *Chem. Commun.*, 2020, **56**, 12037–12040.
29 D. Reta and N. F. Chilton, *Phys. Chem. Chem. Phys.*, 2019, **21**, 23567–23575.
30 W. J. A. Blackmore, G. K. Gransbury, P. Evans, J. G. C. Kragskow, D. P. Mills and N. F. Chilton, *Phys. Chem. Chem. Phys.*, 2023, **25**, 16735–16744.
31 S. Dey, T. Sharma and G. Rajaraman, *Chem. Sci.*, 2024, **15**, 6465–6477.
32 S. K. Gupta, T. Rajeshkumar, G. Rajaraman and R. Murugavel, *Chem. Sci.*, 2016, **7**, 5181–5191.
33 K. Randall McClain, C. A. Gould, K. Chakarawet, S. J. Teat, T. J. Groshens, J. R. Long and B. G. Harvey, *Chem. Sci.*, 2018, **9**, 8492–8503.
34 S. J. Coles, D. R. Allan, C. M. Beavers, S. J. Teat and S. J. W. Holgate, *Struct. Bonding*, Springer, Berlin, Heidelberg, 2020, pp. 1–72.